Immune targeting of fibroblast activation protein triggers recognition of multipotent bone marrow stromal cells and cachexia

Eric Tran,[1] Dhanalakshmi Chinnasamy,[1] Zhiya Yu,[1] Richard A. Morgan,[1] Chyi-Chia Richard Lee,[2] Nicholas P. Restifo,[1] and Steven A. Rosenberg[1]

[1]Surgery Branch and [2]Laboratory of Pathology, National Cancer Institute, National Institutes of Health, Bethesda, MD 20892

Fibroblast activation protein (FAP) is a candidate universal target antigen because it has been reported to be selectively expressed in nearly all solid tumors by a subset of immunosuppressive tumor stromal fibroblasts. We verified that 18/18 human tumors of various histologies contained pronounced stromal elements staining strongly for FAP, and hypothesized that targeting tumor stroma with FAP-reactive T cells would inhibit tumor growth in cancer-bearing hosts. T cells genetically engineered with FAP-reactive chimeric antigen receptors (CARs) specifically degranulated and produced effector cytokines upon stimulation with FAP or FAP-expressing cell lines. However, adoptive transfer of FAP-reactive T cells into mice bearing a variety of subcutaneous tumors mediated limited antitumor effects and induced significant cachexia and lethal bone toxicities in two mouse strains. We found that FAP was robustly expressed on PDGFR-α^+, Sca-1^+ multipotent bone marrow stromal cells (BMSCs) in mice, as well as on well-characterized, clinical-grade multipotent human BMSCs. Accordingly, both mouse and human multipotent BMSCs were recognized by FAP-reactive T cells. The lethal bone toxicity and cachexia observed after cell-based immunotherapy targeting FAP cautions against its use as a universal target. Moreover, the expression of FAP by multipotent BMSCs may point toward the cellular origins of tumor stromal fibroblasts.

CORRESPONDENCE
Eric Tran:
eric.tran@nih.gov
OR
Steven A. Rosenberg:
SAR@mail.nih.gov

Abbreviations used: ACT, adoptive cell therapy; BMSC, BM stromal cell; CAR, chimeric antigen receptor; FAP, fibroblast activation protein; ICS, intracellular cytokine staining; IHC, immunohistochemistry; MSC, mesenchymal stromal cell; OS, osteogenic; PDGFR-α, platelet-derived growth factor receptor-α.

Tumor stromal fibroblasts are the most prominent cell type in the tumor microenvironment of many human cancers such as pancreatic, gastrointestinal, and breast cancers (Feig et al., 2012; Tripathi et al., 2012), although their ontogeny remains incompletely elucidated. Importantly, they appear to play an active role in cancer progression by secreting factors that enhance tumor survival, growth, angiogenesis, and metastasis, in addition to recruiting other tumor-promoting cell types (Feig et al., 2012; Tripathi et al., 2012). Accordingly, many groups have attempted to eradicate transformed cells by targeting fibroblast activation protein (FAP)-expressing stromal cells (Lee et al., 2005; Loeffler et al., 2006; Ostermann et al., 2008; Liao et al., 2009; Santos et al., 2009; Kraman et al., 2010; Wen et al., 2010). FAP is a serine protease implicated in extracellular matrix remodeling (Kelly et al., 2012) and is reported to be strongly expressed by tumor stromal fibroblasts with little to no expression in normal fibroblasts or other normal tissues (Rettig et al., 1988; Garin-Chesa et al., 1990). However, FAP is also expressed in healing wounds and in fibrotic conditions such as fibrosis of the liver and lung, in Crohn's disease, in arthritis, and on various sarcomas (Kelly et al., 2012). The seemingly limited normal tissue expression, and the fact that FAP expression is found in >90% of epithelial cancers (Garin-Chesa et al., 1990), makes FAP an attractive molecule for targeting tumor stromal fibroblasts.

Targeting FAP genetically, or with vaccines or pharmacological agents, has been shown to impair tumor progression in several preclinical cancer models (Lee et al., 2005; Loeffler et al., 2006; Ostermann et al., 2008; Liao et al., 2009; Santos et al., 2009; Kraman et al., 2010; Wen et al., 2010). Unfortunately, targeting FAP in human cancer patients with the monoclonal antibodies F19 and its humanized version Sibrotuzumab (Welt et al., 1994; Hofheinz et al., 2003;

The Rockefeller University Press $30.00
J. Exp. Med. 2013 Vol. 210 No. 6 1125-1135
www.jem.org/cgi/doi/10.1084/jem.20130110

Scott et al., 2003), or the FAP enzyme-inhibitor Talabostat (Narra et al., 2007; Eager et al., 2009a,b), has not demonstrated clinical efficacy. Despite this, favorable biodistribution of the FAP-specific antibodies has been reported, with selective uptake in sites of metastatic disease in patients (Welt et al., 1994; Scott et al., 2003). The general lack of clinical efficacy in these trials could be due to the possibility that binding to or inhibiting FAP activity alone is not sufficient to impact tumor stromal fibroblast function (Kelly et al., 2012).

Adoptive cell therapy (ACT) using ex vivo expanded tumor-infiltrating lymphocytes (TIL) or T cells genetically engineered with antitumor TCRs or chimeric antigen receptors (CARs) can cure some patients with metastatic cancers, demonstrating that T cells can be potent weapons against cancer (Rosenberg, 2012). CARs are typically composed of an extracellular antigen-recognition domain derived from a tumor-reactive monoclonal antibody (scFv) fused to intracellular T cell signaling domains, which, unlike conventional TCRs, allows T cells expressing CARs to directly recognize cell surface proteins and kill target cells in an MHC-independent fashion (Dotti et al., 2009; Sadelain et al., 2009). However, the decision of which antigen to target is a critical parameter of CAR design, as CAR-modified T cells can mediate significant "on-target, off-tumor" toxicities if the antigen being targeted is expressed on normal tissues (Dotti et al., 2009; Sadelain et al., 2009).

In the present study, we tested whether targeting tumor stromal fibroblasts using T cells genetically engineered with FAP-reactive CARs could inhibit tumor growth in various mouse tumor models. We found that adoptive transfer of T cells modified with highly reactive anti-FAP CARs had little impact on tumor progression in a variety of syngeneic mouse tumor implantation models, an observation that could be due to the relatively low stromal content in these tumors. Nonetheless, and more importantly, we found that high doses of FAP-reactive T cells induced severe cachexia and dose-limiting bone toxicity. This toxicity appeared to be the result of T cell targeting of FAP-expressing multipotent BM stromal cells (BMSCs). Thus, FAP is not only expressed by tumor stromal fibroblasts, but also by multipotent BMSCs. The expression of FAP on multipotent BMSCs not only cautions against strategies that can target and destroy FAP-expressing cells, but also may provide biological insight into the cellular origins of tumor stromal fibroblasts.

RESULTS AND DISCUSSION

Expression of FAP by human tumor stromal cells

FAP is reported to be highly expressed on tumor stromal fibroblasts from many different tumor types. Thus, we first assessed the expression of FAP in a variety of human tumors by immunohistochemistry (IHC) using the FAP-specific monoclonal antibody FAP5 (Ostermann et al., 2008). FAP staining was positive in all tumors tested (melanoma, $n = 9$; colorectal, $n = 3$; pancreatic, $n = 3$; and breast, $n = 3$), with the vast majority of samples showing strong FAP staining localized in the fibrotic stromal bands of the tumors (Fig. 1, A–D; and Table S1). In many tumors, thick, intensely FAP-positive stromal bands comprised a large component of the tumor. Thus, in accord with prior reports, FAP is strongly expressed in the reactive stroma of many solid cancers, which makes FAP a potentially attractive antigen for targeting the tumor stroma.

In vitro function of FAP-reactive CARs

To target tumor stromal fibroblasts with T cells, we genetically engineered T cells with CARs specific for FAP. For our preclinical studies, we generated two CAR constructs: (1) FAP5-CAR, which is comprised of the scFv from the FAP-specific antibody FAP5 (Ostermann et al., 2008) used in the aforementioned IHC studies, and is reactive to both mouse and human FAP, and (2) Sibro-CAR, which is comprised of the scFv from Sibrotuzumab, a FAP-reactive antibody that was previously used in clinical trials (Hofheinz et al., 2003; Scott et al., 2003) and is only reactive to human FAP. Both scFv fragments were genetically fused to the CD28, 4-1BB, and CD3-ζ intracellular signaling domains (Fig. 1, E and F; and Tables S2 and S3), and cloned into the MSGV1 retroviral vector. Transduction efficiencies of FAP5-CAR in mouse T cells were between ∼70 and 90% (Fig. 1 G), whereas Sibro-CAR transduced human T cells demonstrated transduction efficiencies between ∼45–65% (Fig. 1 H) as determined by flow cytometry. Both FAP5- and Sibro-CAR–transduced T cells specifically degranulated and produced cytokines when stimulated with plate-bound recombinant FAP or when co-cultured with HEK293 stably expressing FAP, but not when stimulated with irrelevant protein, or when co-cultured with the FAP-negative HEK293 cell line stably expressing eGFP (Fig. 1, I and J for mouse FAP5-CAR; Fig. 1, K and L for human Sibro-CAR). Thus, FAP-reactive CARs were generated and expressed in T cells, and they demonstrated specific in vitro activity.

Attempts to target tumor stromal cells with FAP5-CAR–transduced T cells in vivo

We next tested whether targeting FAP with FAP5-CAR–transduced T cells could mediate antitumor effects in various mouse tumor models. We resorted to the B16 melanoma, MC38 colon cancer, MC17-51 fibrosarcoma, 4T1 breast cancer, CT26 colon cancer, and Renca kidney cancer cell lines, which all did not express FAP in vitro, with the exception of MC17-51, where a small subset of cells demonstrated very low levels of FAP expression (Fig. 2 A). However, when these tumor cells were subcutaneously implanted into syngeneic mice and allowed to grow to treatment size (∼50 mm^2), IHC staining demonstrated FAP positivity in all of these tumors, although the staining intensity was generally much weaker and more diffuse than in human tumors (Fig. 2, B–G, vs. Fig. 1, A–D). Moreover, these murine tumors lacked the thick stromal banding pattern seen in human tumors. The differences in FAP expression level and tumor stromal architecture between these murine tumors and human tumors likely reflects differences in the tumor initiation and development process, in combination with the intrinsic ability of each tumor-cell type to recruit and activate stromal elements. Nonetheless, although weaker, these in vivo murine tumor masses were

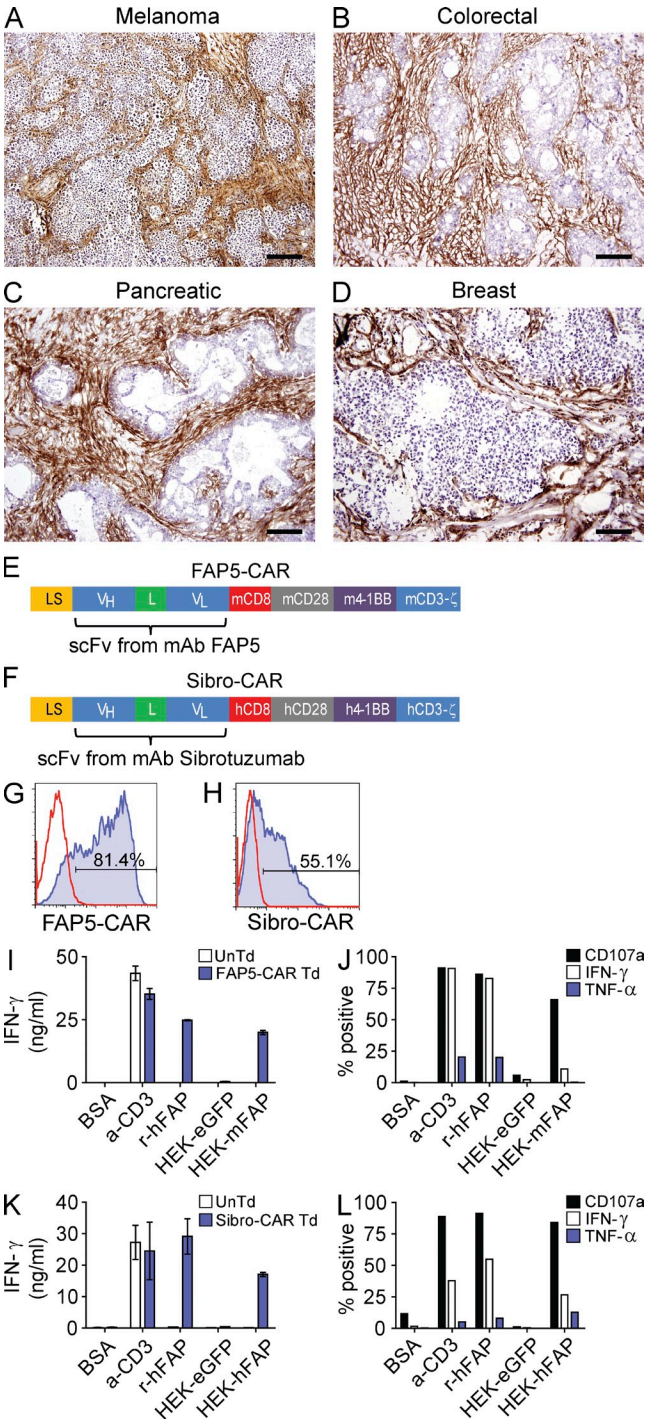

Figure 1. IHC staining for FAP in various human tumors, and design and in vitro activity of FAP-reactive CARs. Representative IHC staining for FAP in human melanoma (A), colorectal (B), pancreatic (C), and breast (D) adenocarcinomas. Isotype stains were negative (not depicted). Bars: 400 µm (A); 200 µm (B–D). Schematic of the FAP-reactive CAR constructs FAP5-CAR (E) and Sibro-CAR (F). LS, GM-CSFR leader sequence; V_H and V_L, variable heavy and light chains; L, 218 linker; CD8, transmembrane domain; CD28, 4-1BB, and CD3-ζ, intracellular signaling domains; m, murine; h, human. Both constructs were cloned into the MSGV1 retroviral vector. Retrovirus containing FAP5-CAR or Sibro-CAR constructs were generated and used to transduce mouse and human T cells, respectively, and flow cytometry was used to assess transduction efficiency at day 2 after transduction for FAP5-CAR (G) and day 8–10 after transduction for Sibro-CAR (H). Solid line is isotype control and filled histogram is FAP5 or Sibrotuzumab stained. Day 5-stimulated untransduced (UnTd) and FAP5-CAR–transduced (Td) mouse T cells were assessed for reactivity against plate-bound BSA, α-CD3 mAb, and recombinant human FAP (r-huFAP), and against HEK293 cell lines expressing or not expressing FAP. After an overnight stimulation, supernatants were assessed for IFN-γ with an IFN-γ ELISA (I), and cells were further assessed for cell surface CD107a expression, and production of IFN-γ and TNF by ICS (J). For ICS, cells are gated on FAP5-CAR Td cells. Day ∼14-stimulated UnTd or Sibro-CAR Td human T cells were assessed for in vitro reactivity as described for mouse. IFN-γ ELISA (K), and ICS results gated on Sibro-CAR Td T cells (L) are shown. Mean ± SD. All results are representative of at least three independent experiments.

generally positive for FAP, and thus we evaluated whether targeting FAP with FAP5-CAR–transduced T cells could inhibit tumor growth in vivo.

To this end, we adoptively transferred FAP5-CAR–transduced or untransduced T cells into lymphodepleted mice bearing established subcutaneous tumors, followed by 6 doses of IL-2. As seen in Fig. 2 H, the antitumor effect of FAP5-CAR–transduced T cells on C57BL/6 mice bearing B16 melanomas was weak. Similar results were seen in C57BL/6 mice bearing MC38 colon cancers (Fig. 2 I), and no antitumor effects were seen in mice bearing MC17-51 fibrosarcomas (Fig. 2 J). Adoptive transfer of FAP5-CAR–transduced T cells also mediated no significant antitumor effects in BALB/c mice bearing 4T1 breast or CT26 colon tumors, and a modest antitumor effect against Renca kidney tumors (Fig. 2, K–M). Thus, in a variety of established, subcutaneous murine tumors, targeting FAP with FAP5-CAR–transduced T cells generally mediated weak antitumor effects at best, although it should be noted that these tumor masses had sparse stroma, and demonstrated only weak to moderate FAP expression.

Transfer of FAP5-CAR–transduced T cells is associated with BM toxicity and cachexia

In addition to the limited antitumor activity of FAP5-CAR–transduced T cells seen in some in vivo tumor models, we also found that infusion of FAP5-CAR–transduced T cells ($1–2 \times 10^7$) led to morbidity or mortality in the majority of these mice (unpublished data). To better understand this toxicity, non–tumor-bearing wild-type C57BL/6 mice were treated with 2×10^7 FAP5-CAR–transduced or untransduced T cells. 7 d later, these mice underwent a comprehensive necropsy by a veterinary pathologist blinded to the treatment conditions. Severe BM hypocellularity and necrosis was seen in mice treated with FAP5-CAR–transduced T cells; this was not seen in mice treated with untransduced T cells (Fig. 3, A and B). Corroborating these pathological observations, the total number of live BM and osteogenic (OS) cells isolated from the femurs and tibias of mice treated with 2×10^7 FAP5-CAR–transduced T cells was drastically diminished compared with

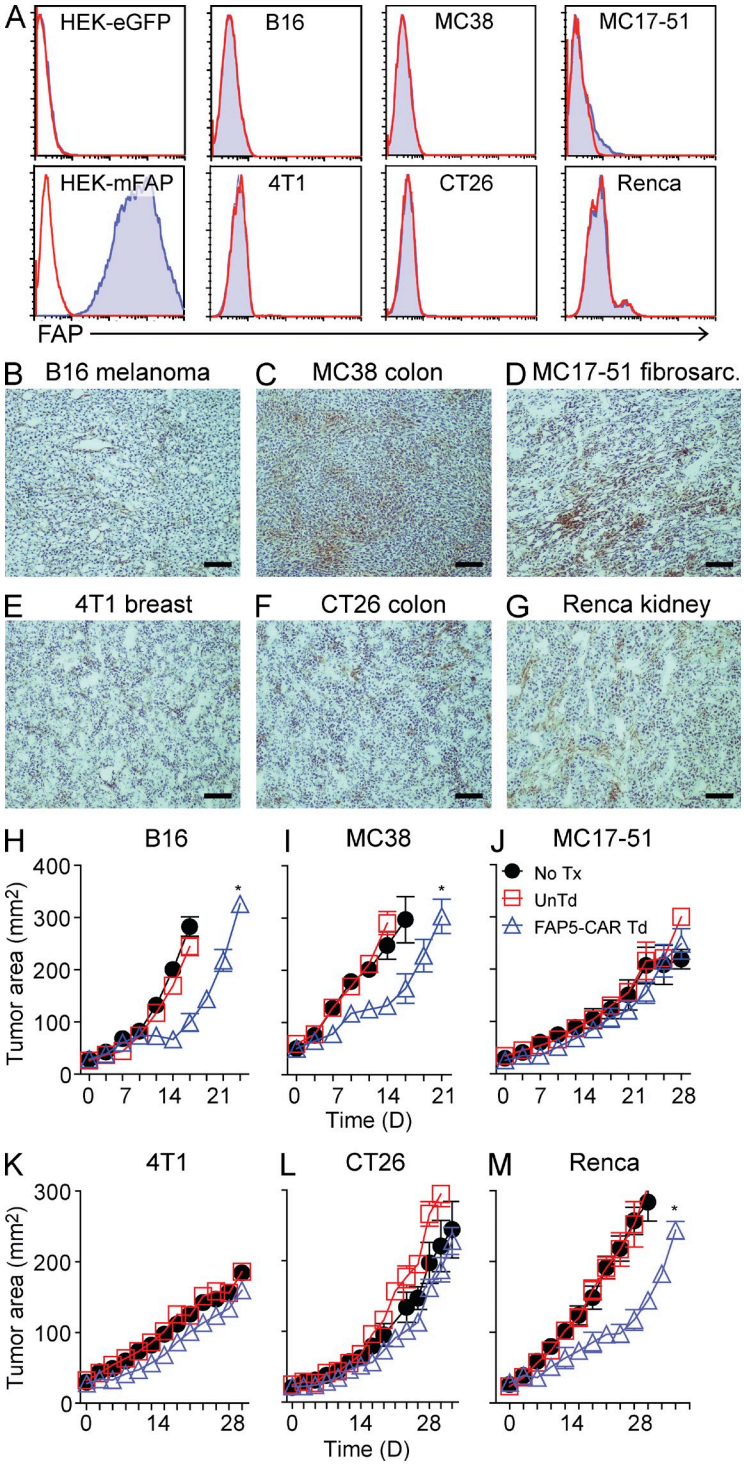

Figure 2. FAP expression in mouse tumors, and in vivo activity of FAP5-CAR–transduced T cells against various murine tumors. In vitro cultured B16, MC38, MC17-51, 4T1, CT26, and Renca murine tumors were assessed for FAP expression by flow cytometry with the FAP-specific antibody FAP5 (A). Solid line is isotype control and filled histogram is FAP5 stained. Results are representative of at least two independent experiments. Established (~11–16 d) subcutaneously implanted B16 (B), MC38 (C), MC17-51 (D), 4T1 (E), CT26 (F), and Renca (G) tumors were harvested from mice (irradiated before harvest) and assessed for FAP expression by IHC using biotinylated-FAP5 antibody. Bars, 400 µm. Representative of at least two independent experiments. C57BL/6 mice bearing established B16 (H), MC38 (I), MC17-51 (J) tumors, and BALB/c mice bearing established 4T1 (K), CT26 (L), or Renca (M) tumors were left untreated (No Tx) or treated with 10^7 UnTd or 10^7 FAP5-CAR Td T cells, and the perpendicular diameters of the tumors were measured over time. Mean ± SEM. Results are representative of at least two independent experiments for H–J and one experiment for K–M with initially five mice per group. *, $P < 0.05$ by Wilcoxon rank-sum test for UnTd versus FAP5-CAR Td T cells.

mice treated with 2×10^7 untransduced T cells (Fig. 3, C and D). In addition to the bone toxicity, mice treated with 2×10^7 FAP5-CAR T cells appeared cachectic and lost ~20% of their body weight by 7 d after treatment (Fig. 3 E).

Mice bearing B16, MC38, MC17-21, 4T1, CT26, and Renca tumors treated with 5×10^6 or 10^7 FAP5-CAR–transduced T cells also lost similar amounts of weight, but the majority of those treated with 5×10^6 FAP5-CAR–transduced T cells did not succumb to treatment-related toxicities (unpublished data). Nonirradiated, lymphoreplete mice receiving high doses of FAP5-CAR–transduced T cells also suffered from similar bone toxicities and cachexia (Fig. 3, C, D, and F).

These toxicities were not limited to non–tumor-bearing mice and mice bearing tumors with low FAP expression, as the adoptive transfer of FAP5-CAR–transduced T cells into *Rag1*-deficient mice bearing a stroma-rich, intensely FAP-positive

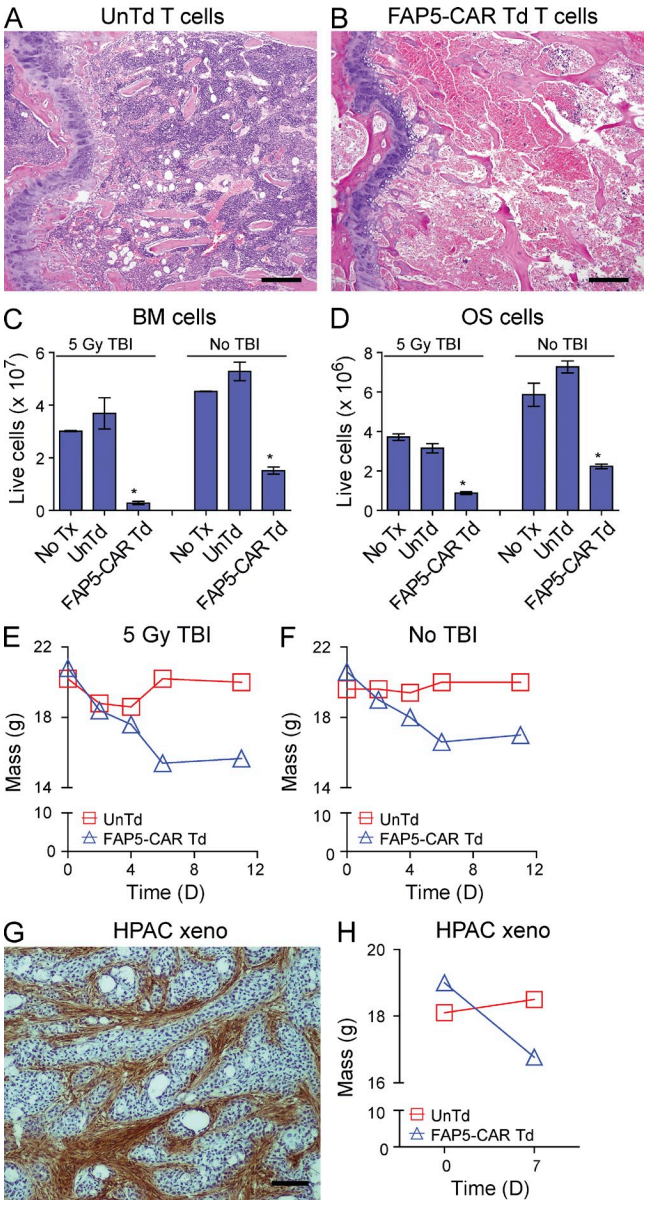

Figure 3. Bone toxicity and cachexia in mice treated with FAP5-CAR T cells. Irradiated mice were treated with 2 × 10^7 UnTd or FAP5-CAR Td T cells, and 7 d later subjected to a comprehensive necropsy. H&E-stained cross section of the femurs from mice treated with UnTd (A) or FAP5-CAR Td (B) T cells. Bars, 400 µm. Femurs and tibias of irradiated and nonirradiated mice that did not undergo adoptive cell transfer (No Tx) or that underwent adoptive transfer with UnTd or FAP5-CAR Td T cells were harvested at day 7 (2 mice pooled per group), and BM (C) and OS (D) cells were isolated and live cells quantitated. Mean ± SD. Data are the average number of cells isolated from the femurs and tibiae of one mouse, and are representative of at least two independent experiments. *, $P < 0.01$ compared with UnTd and No Tx in their respective group, by two tailed Student's *t* test. Average weights of irradiated (E) or nonirradiated (F) mice treated with 2 × 10^7 UnTd or FAP5-CAR Td T cells (5 mice per group). Results are representative at least three independent experiments. *Rag1*-deficient mice bearing the human pancreatic cancer xenograft HPAC were sacrificed between days 18–21 and tumors were harvested and assessed for FAP expression by IHC using biotinylated-FAP5 (G). Bar, 400 µm. Representative of at least two independent experiments. *Rag1*-deficient mice bearing established HPAC tumors (50–70 mm^2) were treated with 10^7 UnTd or FAP5-CAR Td mouse T cells. Shown are weights on day 0 and day 7 (H). Mean ± SEM. Each group initially contained five mice. Similar results were seen in mice treated with 5 × 10^6 FAP5-CAR Td T cells in three independent experiments.

pancreatic cancer xenograft (Fig. 3 G) also led to cachexia and significant morbidity (Fig. 3 H and not depicted). Thus, FAP-reactive T cells can induce major toxicities in both the absence and presence of a highly FAP-positive tumor stroma.

Mouse and human multipotent BMSCs express FAP

The observed bone toxicity suggested that the FAP5-CAR–transduced T cells were targeting some aspect of bone. Given that most, if not all, cells of hematopoietic origin do not express FAP (Bae et al., 2008), it was unlikely that direct targeting of hematopoietic cells by FAP5-CAR–transduced T cells was responsible for the bone toxicity. Thus we tested whether FAP5-CAR–transduced T cells were targeting other non-hematopoietic compartments of bone. To that end, we first assessed the expression of FAP on freshly isolated BM and OS cells from the tibias and femurs of mice. As expected, BM and OS cells of hematopoietic or erythroid origin (Lin^+ cells: $CD45^+$/$TER119^+$) were largely FAP^- (Fig. 4, A and B). However, in contrast, OS cells of nonhematopoietic origin (Lin^- cells: $CD45^-$/$TER119^-$) were markedly enriched in FAP^+ cells (Fig. 4 B). Given that multipotent, mesenchymal BMSCs are known to be enriched in Lin^- OS cells, we stained OS cells with antibodies specific for PDGFR-α and Sca-1, which are markers ascribed to murine multipotent BMSCs (Morikawa et al., 2009), and found that cells that co-expressed these markers were uniformly positive for FAP (Fig. 4 B). Cells expressing PDGFR-α alone were also uniformly FAP^+, whereas the Sca-1 single-positive, and Sca-1/PDGFR-α double-negative populations displayed more heterogeneous expression of FAP (Fig. 4 B). Thus, freshly isolated OS cells of nonhematopoietic origin, including multipotent BMSCs, express FAP and therefore may potentially be targeted by FAP5-CAR–transduced T cells.

To assess the impact of FAP5-CAR–transduced T cells on FAP^+ OS cells in vivo, we adoptively transferred 2 × 10^7 FAP5-CAR–transduced or untransduced T cells into mice. 7 d later, we assessed FAP expression on various populations of freshly isolated OS cells. As shown in Fig. 4, C and D, there was a marked decrease in FAP expression in the OS cell populations isolated from mice treated with FAP5-CAR–transduced T cells compared with mice treated with untransduced T cells. This was associated with a concomitant decrease in the mean fluorescence intensity (MFI) of FAP in these populations, with the greatest fold decrease consistently seen in the PDGFR-α single-positive, and multipotent Sca-1/PDGFR-α double-positive cell populations (Fig. 4 E). Thus, the adoptive transfer of FAP5-CAR–transduced T cells in mice is associated with a loss of OS cells expressing high levels of FAP.

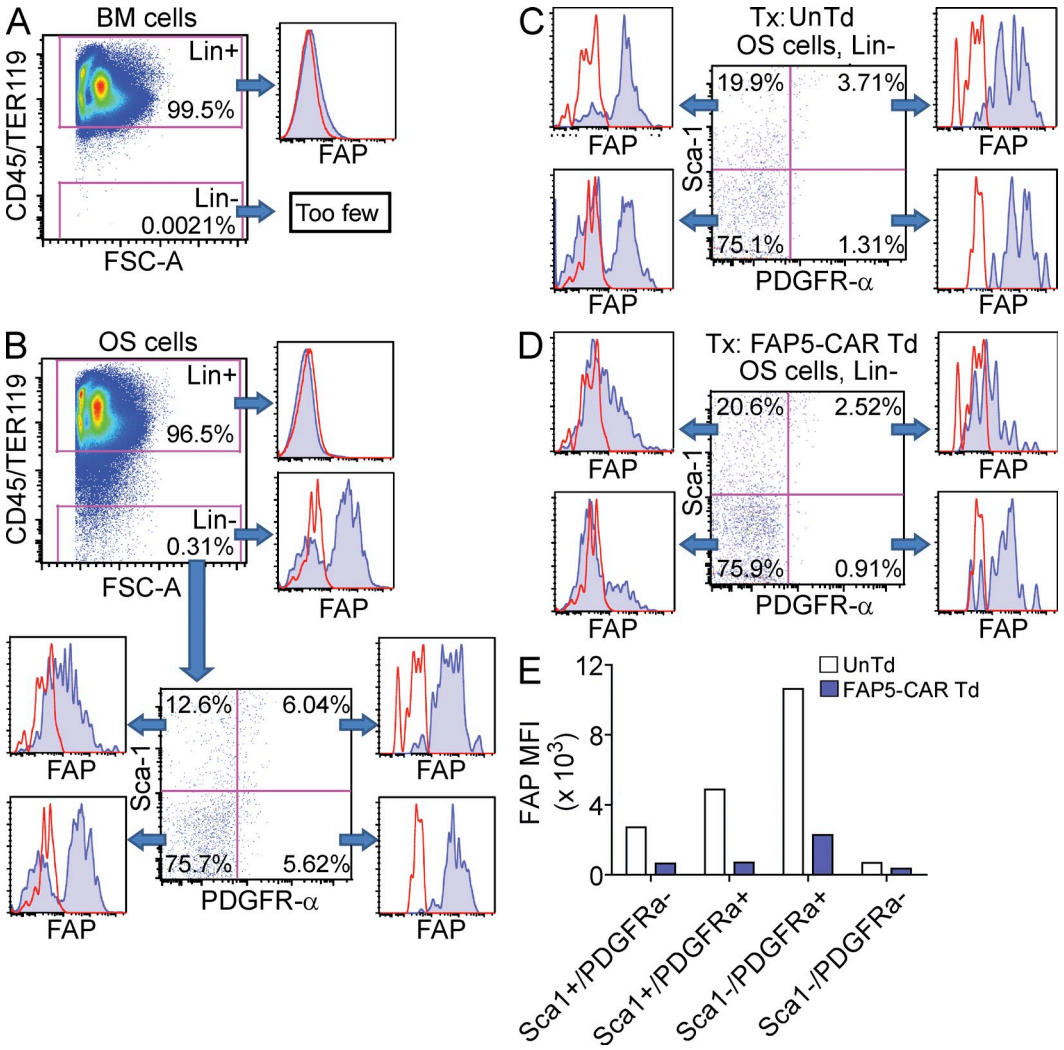

Figure 4. Expression of FAP on freshly isolated murine BMSCs from OS cells. BM (A) and OS cells (B) were isolated from untreated wild-type C57BL/6 mice and stained with antibodies against CD45, TER119, Sca-1, PDGFR-α, and FAP, followed by flow cytometry analysis. $CD45^+/TER119^+$ cells demarcate hematopoietic and erythroid lineage cells (Lin^+). Expression of FAP in various populations of OS cells stained with antibodies specific for Sca-1 and PDGFR-α (B). Irradiated non–tumor-bearing mice were treated with 2×10^7 UnTd or FAP5-CAR Td T cells and, 7 d later, OS cells were isolated and analyzed as in B. Expression of FAP on various OS cell populations isolated from mice treated with UnTd (C) or FAP5-CAR Td (D) T cells is shown. (E) Mean fluorescence intensity (MFI) of FAP in the various Sca-1 and PDGFR-α subsets found in OS cells. All data are gated on live, single cells. Data for C–E are further gated on Lin^- ($CD45^-/TER119^-$) cells. Solid lines are isotype controls and filled histograms are FAP5 stained. All data are representative of at least two independent experiments.

Since multipotent BMSCs provide essential environmental support for hematopoiesis by secreting factors that promote the maintenance of hematopoietic stem cells (Méndez-Ferrer et al., 2010; Ding et al., 2012), and by differentiating into key niche elements such as osteoblasts, adipocytes, chondrocytes, and CXCL12-abundant reticular cells (Nombela-Arrieta et al., 2011), their destruction may contribute to the observed bone toxicity. Therefore, we next tested whether FAP5-CAR–transduced T cells could directly recognize BMSCs in vitro. Cultured murine BMSCs (passage 5) were first assessed for FAP expression by flow cytometry. As seen in Fig. 5 A (left), some of these murine BMSCs expressed FAP and, consistent with the aforementioned results, the Sca-1/PDGFR-α double-positive population displayed uniform expression of FAP (Fig. 5 A, middle and right). Importantly, co-culture assays revealed that these murine BMSCs were specifically recognized by FAP5-CAR–transduced T cells (Fig. 5, B and C). We also assessed FAP expression on highly pure, well-characterized, clinical-grade multipotent human BMSCs from three different donors (Fig. 5 D). Multipotent BMSCs from all three donors were uniformly and strongly FAP-positive as determined by flow cytometry with the two FAP-specific antibodies Sibrotuzumab and FAP5 (Fig. 5, E and F). Similar to mouse, human T cells transduced with the human FAP–reactive Sibro-CAR

degranulated and produced effector cytokines upon co-culture with human BMSCs (Fig. 5, G and H). Thus, both murine and human multipotent BMSCs express FAP and can be targeted by FAP-CAR–transduced T cells.

Given that FAP is expressed on multipotent BMSCs, which are essential for hematopoiesis, it is intriguing that no significant toxicities were reported in previous preclinical studies targeting FAP (Lee et al., 2005; Loeffler et al., 2006;

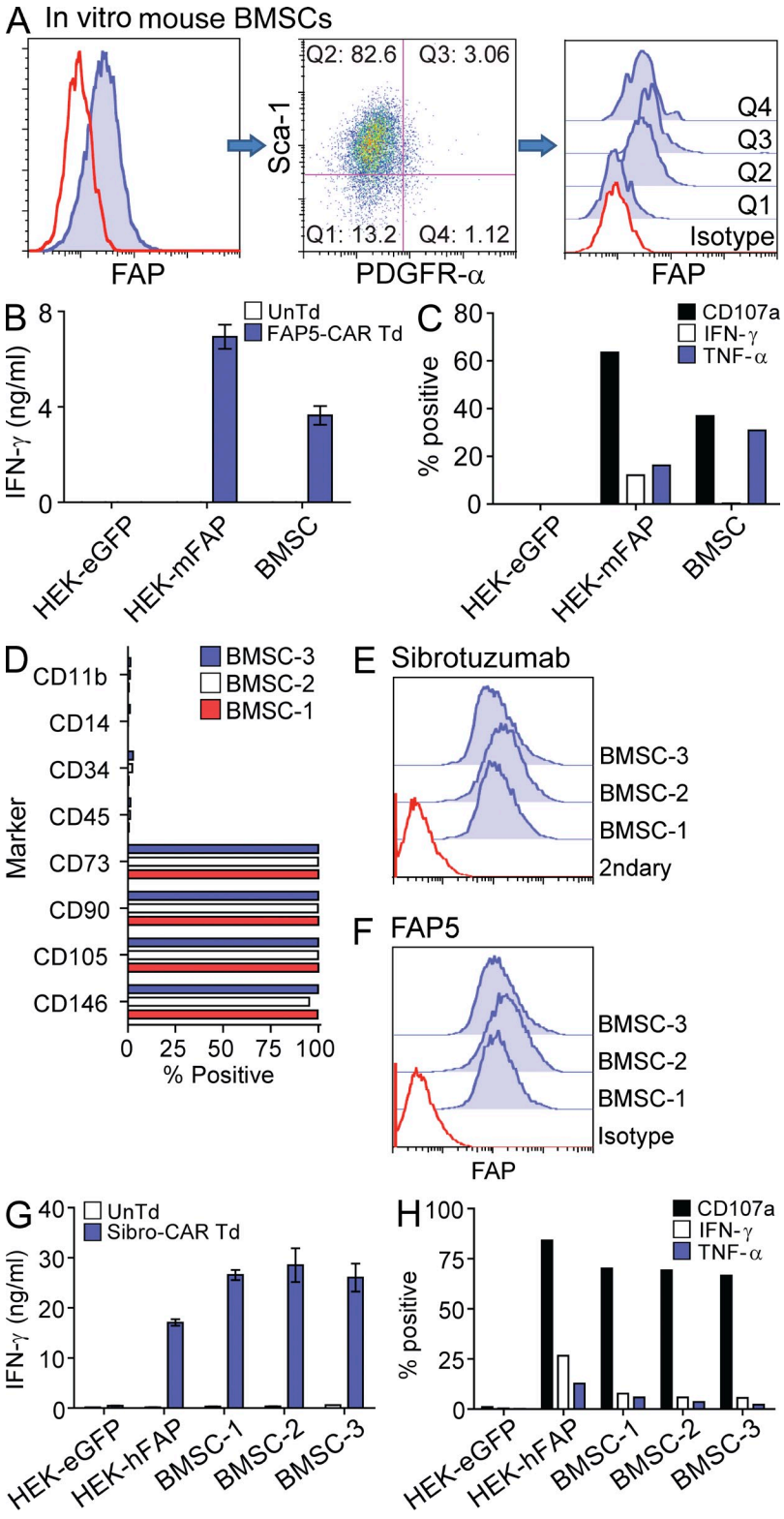

Figure 5. Murine and human multipotent BMSCs express FAP and are recognized by T cells expressing FAP-reactive CARs. Passage-5 in vitro–expanded murine BMSCs were stained with antibodies specific for Sca-1, PDGFR-α, and FAP, and assessed by flow cytometry (A). "Q" represents quadrant. Solid lines are isotype controls and filled histograms are FAP stained. UnTd or FAP5-CAR Td T cells were cultured overnight with murine BMSCs and supernatants were assessed for IFN-γ by ELISA (B), and cells were further analyzed for expression of CD107a and production of IFN-γ and TNF by ICS (C). Mean ± SD. Data are representative of two independent experiments. Flow cytometric phenotype of in vitro–expanded human BMSCs derived from three different donors (D). BMSCs from D were stained with the FAP-specific monoclonal antibodies Sibrotuzumab (E) and FAP5 (F) and assessed by flow cytometry. Solid lines are isotype or secondary antibody controls and filled histograms are FAP or Sibrotuzumab stained. UnTd or Sibro-CAR Td T cells were cultured overnight with BMSCs and the supernatants assessed for IFN-γ by ELISA (G), and cells were further analyzed for CD107a expression and IFN-γ and TNF production by ICS (H). Mean ± SD. Similar results were seen with two additional T cell donors.

Ostermann et al., 2008; Liao et al., 2009; Santos et al., 2009; Kraman et al., 2010; Wen et al., 2010). Perhaps this discrepancy reflects differences in the potency and/or mechanism of the various FAP-targeting therapies. For example, the antitumor T cell response mediated by adoptively transferred T cells is more robust than that induced by vaccines. It is also possible that there is differential processing and presentation of FAP epitopes in tumor stromal fibroblasts compared with BMSCs, which may allow T cells induced by vaccines to specifically target tumor stromal fibroblasts and not BMSCs. This scenario would not be present in FAP-CAR–transduced T cells, which by design, directly recognize cell surface FAP in an MHC-independent fashion.

In addition to residing in bone, where they are called BMSCs, multipotent mesenchymal stromal cells (MSCs) are found throughout the body, including tissues of mesodermal origin such as adipose tissue, muscle, and tendon (Nombela-Arrieta et al., 2011). There is also evidence showing that MSCs can be found in almost all adult tissues (da Silva Meirelles et al., 2006). The expression of FAP on MSCs in a wide range of tissues could explain some of the other toxicities seen in mice treated with FAP5-CAR–transduced T cells. For example, mice treated with FAP5-CAR–transduced T cells were cachectic (Fig. 3, E, F, and H). Although the cachexia could be a consequence of the bone toxicity, it's also possible that the FAP-reactive T cells were targeting other cells that express FAP, such as MSCs in adipose tissue or muscle. Since adipose tissue is a rich source of MSCs, their targeting could contribute to the observed weight loss. Consistent with this, we found that stromal cells isolated from mouse adipose tissues were FAP-positive as determined by flow cytometry (unpublished data), and moreover, pathological assessment revealed scant adipose stores in mice treated with FAP5-CAR–transduced T cells. Additionally, recent data from a transgenic mouse model that allows the bioluminescence imaging of FAP-positive cells demonstrates that FAP-positive cells are indeed found in most normal tissues (unpublished data). Thus, expression of FAP on MSCs residing in bone, adipose, and perhaps other tissues likely explain the spectrum of toxicities seen in mice treated with FAP5-CAR–transduced T cells.

The finding that FAP is robustly expressed by multipotent BMSCs (Fig. 4 and 5; Bae et al., 2008) and MSCs residing in other normal tissues raises safety concerns for therapies that aim to target and destroy FAP-positive tumor stromal cells. However, there are some malignancies where direct targeting and perturbation of the BM niche may be desirable. For example, in multiple myeloma and neoplasms of lymphoid and myeloid origin, BMSCs can play a critical role in supporting neoplastic cell growth and survival in the BM (Tripodo et al., 2011), and thus their targeting may be of therapeutic value. However, any potential antitumor benefit gained by targeting BMSCs with FAP-reactive T cells would have to be carefully weighed with the ensuing hematological toxicity and cachexia.

Finally, our findings may shed some light onto the biology of a key immunosuppressive element of the tumor stroma. The cellular origins of tumor stromal fibroblasts are incompletely elucidated and our finding that FAP is expressed by both tumor stromal fibroblasts and multipotent BMSCs is consistent with the idea that BMSCs may be a source of tumor stromal cells (Mishra et al., 2008). It seems plausible that some tumor stromal cells may simply be multipotent MSCs recruited into the tumor microenvironment, and thus the promising strategy of targeting these normal tumor components must be approached with great care to avoid potentially life threatening collateral damage to these essential regenerative cells.

MATERIALS AND METHODS

Ethics statement. All patient-derived material used in this study was approved by the Institutional Review Board of the National Cancer Institute (NCI). All animal studies were performed in accordance with the Animal Care and Use Committee guidelines of the National Institutes of Health and were conducted under protocols approved by the Animal Care and Use Committee of the NCI.

IHC. Human melanoma and mouse tumors were embedded in OCT compound (Tissue-Tek) and frozen at −80°C before sectioning onto positively charged slides. Frozen human breast, colorectal, and pancreatic tumor slides were provided by the Cooperative Human Tissue Network, which is funded by the NCI. Tissue sections were stained using standard IHC procedures. In brief, slides were air dried for 20 min, and then fixed with cold acetone for 10 min at 4°C. Sections were then air dried (20 min), washed with PBS (three times), and incubated with 0.3% hydrogen peroxide for 10 min to block endogenous peroxidase. After PBS wash (two times), sections were blocked with protein block solution (Dako), washed with PBS (two times), and then further blocked with Biotin/Avidin block reagent (Invitrogen). After PBS wash (three times), sections were incubated with primary antibody or isotype control antibody for 45 min at room temperature in a humidified chamber. For human tissues, the FAP-specific antibody FAP5 (Ostermann et al., 2008) or mouse IgG2a isotype control antibody (BioLegend) were used at 0.625 µg/ml, and developed with the mouse Dako EnVision+ System-HRP (DAB) kit as recommended. For mouse tissues, FAP5 or mouse IgG2a isotype control antibodies were biotinylated (EZ-Link NHS PEG4-biotin; Thermo Fisher Scientific) and used at ∼2 µg/ml. Sections were developed with ABC reagent (Vector Laboratories) and DAB substrate (Dako). All slides were counterstained with hematoxylin, washed, dehydrated through graded alcohol and xylene, and then mounted. Stained human tissue sections were evaluated by a pathologist for: % stroma (of tumor section), % stromal cells positive for FAP (either >50% or <50%), and FAP staining intensity (0 = no staining, 3+ = strong staining).

Cell lines and media. The tumor cell lines B16-F10 (mouse melanoma), MC17-51 (mouse fibrosarcoma), 4T1 (mouse mammary carcinoma), CT26 (mouse colon adenocarcinoma), Renca (mouse renal adenocarcinoma), and HPAC (human pancreatic adenocarcinoma) were maintained in RPMI supplemented with 10% heat-inactivated FBS (Sigma-Aldrich), 100 U/ml penicillin, 100 µg/ml streptomycin, 2 mM L-glutamine, and 25 mM Hepes buffer (all from Invitrogen). The mouse colon adenocarcinoma MC38 and the retrovirus packaging line 293GP were maintained in DMEM (Quality Biologics Inc.) with the same supplements as described for RPMI.

To generate FAP-expressing cell lines, FAP-negative HEK293 cells were transduced with retrovirus encoding mouse or human FAP cDNA (Open Biosystems), or eGFP as control. All cloning was done using the Fast Cloning Pack and FastDigest restriction enzymes (both from Fermentas). The DNA sequence of mouse and human FAP was verified by standard Sanger sequencing (Macrogen). Retroviral supernatants were made and used to transduce HEK293 cell (described in following section). Transduced HEK293 cells were selected with 1 mg/ml G418 (CellGro). HEK293 cells stably expressing eGFP, mouse FAP, or human FAP are designated as HEK-eGFP, HEK-mFAP, and HEK-hFAP, respectively.

Mouse T cell media composed of RPMI containing 10% heat-inactivated FBS (Sigma-Aldrich), 100 U/ml penicillin, 100 µg/ml streptomycin, 0.05 mM 2-mercaptoethanol, 0.1 mM MEM nonessential amino acids, 1 mM sodium pyruvate, and 2 mM L-glutamine (all from Invitrogen), and 60 IU/ml of rhIL-2 (Chiron). Human T cell media was comprised of RPMI supplemented with 10% heat-inactivated human AB serum (Gemini Bio-Products), 2 mM L-glutamine, 100 U/ml penicillin, 100 µg/ml streptomycin, 10 µg/ml gentamicin (Lonza or CellGro), 1 mM sodium pyruvate, and 300 IU/ml rhIL-2 (Chiron).

BMSCs (passage 5) derived from C57BL/6 mice were obtained from the Texas A&M Institute for Regenerative Medicine and cultured in Iscove's modified Dulbecco medium (IMDM) supplemented with 10% FBS (Sigma-Aldrich), 10% horse serum, 100 U/ml penicillin, 100 µg/ml, streptomycin, 0.25 µg/ml amphotericin B, and 2 mM L-glutamine. Human clinical-grade BMSCs were generated by the National Institutes of Health Department of Transfusion Medicine, as previously described (Sabatino et al., 2012), and cultured in α-MEM (Lonza) supplemented with 20% FBS (Sigma-Aldrich) and 10 µg/ml gentamicin (Lonza).

Generation of mouse and human FAP-CARs, retrovirus production, and T cell transduction. The CAR constructs used in this study are illustrated in Fig. 1 (E and F). The mouse and human FAP-specific scFv used for generating the FAP5-CAR was derived from the high affinity mouse antibody FAP5 (Ostermann et al., 2008), which has a Kd of 0.6 and 5 nM for mouse and human FAP, respectively. The high-affinity (6 nM) human FAP-specific scFv used for generating Sibro-CAR was derived from the monoclonal antibody Sibrotuzumab (BIBH1; Scott et al., 2003). The scFv sequences of FAP5 and Sibrotuzumab were obtained from US Patent Application Publications US 2009/0304718 A1 and US 2003/0103968 A1, respectively. After codon optimization and synthesis (Blue Heron Technology), the scFv constructs were cloned in-frame into the MSGV1 retroviral vector containing the CD8α-chain hinge, and the CD28, 4-1BB, and CD3-ζ intracellular signaling domains. All CAR constructs were sequence verified (Macrogen). The complete genetic sequence of the FAP5-CAR and Sibro-CAR are shown in Tables S2 and S3, respectively.

Transient retroviral supernatants were generated by co-transfecting 293GP cells (6×10^6 cells plated on 10-cm poly-D-lysine–coated plates 1 d before transfection) with the MSGV1 FAP-CAR plasmid (9 µg/plate) and the appropriate envelope encoding plasmid (ECO for mouse and RD114 for human; 4.5 µg/plate) using Lipofectamine 2000 (Invitrogen). Retroviral supernatants were collected at ∼48 h after transfection and centrifuged onto Retronectin-coated (10 µg/ml; Takara), non–tissue culture–treated 6-well plates at 2,000 g for 2 h at 32°C. Activated T cells (2×10^6 per well, at 0.5×10^6 cells/ml in IL-2 containing T cell media) were then spun onto the retrovirus plates for 10 min at 300 g. Activated T cells were transduced overnight, removed from the plates and further cultured in IL-2 containing T cell media until required. To generate activated mouse T cells for transduction, spleens from littermate mice were crushed through a 40-µM cell strainer (BD) followed by red cell lysis with ACK buffer (Lonza). Mouse T cells were then enriched using the Dynal Mouse T cell Negative Isolation kit (Invitrogen). $CD3^+$ cells (2×10^6 cells/ml) were then stimulated with 2 µg/ml ConA (Sigma-Aldrich), 60 IU/ml rhu IL-2 (Chiron), and 1 ng/ml recombinant mouse IL-7 (R&D Systems) for 2 d before transduction. Murine cells stimulated this way were consistently ∼90% $CD3^+CD8^+$ on the day of adoptive transfer. To generate activated human T cells for transduction, pheresis samples (2×10^6 cells/ml) from metastatic melanoma patients were stimulated with 50 ng/ml soluble OKT3 antibody and 300 IU/ml recombinant human IL-2 (Chiron) for two days before transduction. After transduction, cells were further cultured in human T cell media supplemented with 300 IU/ml of IL-2 until required (typically ∼2 wk).

Cell surface flow cytometry. Cell surface expression of mouse FAP was detected using the monoclonal antibody FAP5 (MFP5; Ostermann et al., 2008) at 2.5 µg/ml, and human FAP was detected using FAP5 and/or Sibrotuzumab (BIBH1; Scott et al., 2003) at 2.5 µg/ml. Both antibodies were provided by P. Garin-Chesa (Boehringer Ingelheim, Vienna, Austria). The secondary detection antibody was PE-conjugated AffiniPure F(ab')2 fragment donkey anti–mouse IgG, and PE-conjugated AffiniPure F(ab')2 fragment donkey anti–human IgG (both from Jackson ImmunoResearch Laboratories) used at 1:100 dilution to detect the FAP5 and Sibrotuzumab antibodies, respectively. All FAP staining experiments contained a negative control (HEK-eGFP) and positive control (HEK-mFAP or HEK-hFAP) cell line. Mouse IgG2a isotype antibody was used as a control for FAP5 antibody in indicated experiments. To detect FAP5-CAR expression on mouse T cells, T cells were stained with the biotin-SP–conjugated AffiniPure goat anti–mouse IgG F(ab)2 fragment specific antibody (Jackson ImmunoResearch Laboratories) at 1:20 dilution, followed by 2.5 µg/ml streptavidin-PE (BD). To detect Sibro-CAR expression on human T cells, T cells were stained with 2 µg/ml C-terminal His-tagged recombinant human FAP (GenWay Biotech Inc.) followed by 1:10 dilution of PE-conjugated anti-His antibody (Miltenyi Biotec). The following antibodies were used for staining of BM and OS cells: 0.15 µg/ml CD45-PE, 1.25 µg/ml TER119-PE, 5 µg/ml PDGFR-α-APC, and 1 µg/ml Sca-1-PE-Cy7 (all from eBioscience, except Sca-1-PE-Cy7 [BD]), and biotinylated FAP5 antibody (5 µg/ml, described above) with the secondary detection reagent Alexa Fluor 488–conjugated streptavidin (2 µg/ml, Invitrogen). The following isotype controls were used at the same concentrations as the corresponding test antibodies: PE-rat IgG2b, APC-rat IgG2a, and PE-Cy7 rat IgG2a (all from eBioscience), and biotinylated mouse IgG2a (control for biotinylated FAP5). For all flow cytometry experiments, cells were stained for 20–30 min at 4°C in the dark and washed two times with flow cytometry buffer (1X PBS + 1% FBS). For BM and OS cells, cells were additionally blocked with mouse Fc block (10–20 µg/ml; BD) before antibody staining. Cells were stained with propidium iodide (PI) to demarcate live/dead cells before acquisition on either a FACSCalibur or a FACSCanto II (BD). Data were analyzed with FlowJo software (Tree Star).

T cell assays. FAP-CAR–transduced T cells were assessed for reactivity against the target antigen FAP by assessing culture supernatants for IFN-γ using IFN-γ ELISA, and by analyzing the cells using a flow cytometry-based degranulation/intracellular cytokine staining (ICS) assay. For plate-bound stimulations, 96-well flat bottom plates were coated overnight at 4°C with 1 µg/ml BSA, 1 µg/ml recombinant human FAP (GenWay Biotech or R&D Systems), 1 µg/ml anti–mouse CD3-ε antibody (clone 145-2C11; BioLegend), or 1 µg/ml OKT3 (Orthoclone), all diluted in PBS. For plate-bound antigen stimulation assays, cells were plated at 10^5 cells per well in 200 µl of media. For most co-culture experiments, 10^5 T cells were cultured with 10^5 target cells in 200 µl of media. For human co-culture experiments involving BMSCs, 3×10^5 T cells were cultured with 10^5 BMSCs in a 48-well plate (in 500 µl total volume). All T cell assays were conducted using media without IL-2. In select experiments, fluorochrome-conjugated anti-CD107a antibody was added to the wells at the beginning of the stimulation; for mouse, anti-CD107a-Alexa Fluor 647 (BioLegend) was used at 1.25 µg/ml and for human, anti-CD107a-FITC (BD) used at 20 µl antibody per ml of culture. At 20–22 h after stimulation, both GolgiStop and GolgiPlug (BD) were added to cultures (each used at 1/2 the recommended dilution). After 4–6 h, supernatants were harvested and used in IFN-γ ELISAs (eBioscience), and cells were further processed for ICS. In brief, cells were harvested, stained for FAP-CAR (described above) and then fixed, permeabilized, and stained using the BD Cytofix/Cytoperm kit as directed. Mouse cells were stained with 5 µg/ml anti–mouse IFN-γ-FITC (BioLegend) and 4 µg/ml anti–mouse TNF-PerCP/Cy5.5 (BD). Human cells were stained with 1.25 µg/ml anti–human IFN-γ-Alexa Fluor 647 (BioLegend) and 2.5 µl/100 µl anti–human TNF-PerCP/Cy5.5 (BD).

In vivo experiments. Inbred female C57BL/6 mice were purchased from the National Cancer Institute–Frederick Cancer Research and Development Center (Frederick, MD). Female and male BALB/cJ, and female *Rag1*-deficient mice were purchased from The Jackson Laboratory. In adoptive cell transfer (ACT) models with syngeneic tumors, 8–12-wk-old mice were injected subcutaneously with 5×10^5 tumor cells and ∼11 d later, when

tumors were typically 30–60 mm^2, mice were lymphodepleted with 5 Gy total body irradiation, and then treated with T cells via tail vein injection. For human pancreatic cancer xenograft experiments, *Rag1*-deficient mice were injected subcutaneously with 1.5–2 × 10^6 HPAC cells and then ∼21 d later, when tumors were typically 50–70 mm^2, were treated with T cells via tail vein injection. All mice receiving T cells were also given intraperitoneal injections of rhIL-2 b.i.d. (2.2 × 10^5 IU/dose) for 6 doses total. Unless otherwise indicated, at least two independent experiments were performed with similar results. As a quality control, T cells used in every ACT experiment were assessed for FAP5-CAR expression and specific in vitro activity (see T cell assays). In all ACT experiments, the adoptively transferred T cells demonstrated >70% transduction efficiency of the FAP5-CAR and specifically recognized plate-bound FAP and FAP-expressing cells. All experiments were performed in a blinded, randomized fashion, with each treatment group including a minimum of 5 mice. Blinded tumor measurements are the products of perpendicular diameters and are plotted with ± SEM. Tumor growth statistics were calculated using the Wilcoxon rank-sum test, based on linear slopes of the tumor growth curves at each data point. P-values of 0.05 or lower were considered significant.

Isolation of BM and OS cells. The protocol used was derived from StemCell Technologies website. In brief, mice were sacrificed and femurs and tibias were harvested and cleaned of muscle. Epiphyses were removed with a scalpel and bones were further scraped clean using the scalpel. Cleaned bones were placed in a mortar containing cold buffer (PBS + 2% FBS + 1 mM EDTA). Bones were then very gently crushed with a pestle to release the BM, which was collected and filtered through a 70-µM strainer. To isolate OS cells, the bone fragments were washed multiple times with buffer and gentle agitation (approximately three to six times, or until the buffer is no longer red/pink), and then minced with a scalpel into 1–2-mm pieces in the presence of 0.25% collagenase I (Invitrogen) solution (in PBS + 20% FBS). Bones were digested in the 0.25% collagenase solution (5 ml per mouse) for 45 min in a 37°C shaking incubator, and then filtered through a 70-µM strainer and washed with cold buffer. Red blood cells in BM and OS were lysed with ACK buffer and washed. Cells were then counted using a hemocytometer with Trypan blue exclusion, and then stained for flow cytometry analysis as described in the Cell Surface Flow Cytometry section above.

We would like to thank Pilar Garin-Chesa (Boehringer Ingelheim) for kindly providing the FAP5 (MFP5) and Sibrotuzumab (BIBH1) antibodies. We thank Dave Jones and Zulmarie Franco for excellent assistance in animal studies and the Division of Veterinary Resources (National Institutes of Health), and the NCI-Frederick Pathology/Histotechnology Laboratory for help with mouse pathology. Human BMSCs were a generous gift from Pamela Robey, David Stroncek, Marianna Sabatino, Jiaqiang Ren, and the NIH BMSC Transplantation Center. We also thank Pamela Robey, Christian Hinrichs, and Luca Gattinoni for helpful discussions.

This research was supported by the Intramural Research Program of the NIH and NCI.

The authors have no conflicts of interest.

Submitted: 14 January 2013
Accepted: 8 May 2013

REFERENCES

Bae, S., C.W. Park, H.K. Son, H.K. Ju, D. Paik, C.J. Jeon, G.Y. Koh, J. Kim, and H. Kim. 2008. Fibroblast activation protein alpha identifies mesenchymal stromal cells from human bone marrow. *Br. J. Haematol.* 142:827–830. http://dx.doi.org/10.1111/j.1365-2141.2008.07241.x

da Silva Meirelles, L., P.C. Chagastelles, and N.B. Nardi. 2006. Mesenchymal stem cells reside in virtually all post-natal organs and tissues. *J. Cell Sci.* 119:2204–2213. http://dx.doi.org/10.1242/jcs.02932

Ding, L., T.L. Saunders, G. Enikolopov, and S.J. Morrison. 2012. Endothelial and perivascular cells maintain haematopoietic stem cells. *Nature.* 481: 457–462. http://dx.doi.org/10.1038/nature10783

Dotti, G., B. Savoldo, and M. Brenner. 2009. Fifteen years of gene therapy based on chimeric antigen receptors: "are we nearly there yet?". *Hum. Gene Ther.* 20:1229–1239. http://dx.doi.org/10.1089/hum.2009.142

Eager, R.M., C.C. Cunningham, N. Senzer, D.A. Richards, R.N. Raju, B. Jones, M. Uprichard, and J. Nemunaitis. 2009a. Phase II trial of talabostat and docetaxel in advanced non-small cell lung cancer. *Clin. Oncol. (R Coll Radiol).* 21:464–472. http://dx.doi.org/10.1016/j.clon.2009.04.007

Eager, R.M., C.C. Cunningham, N.N. Senzer, J. Stephenson Jr., S.P. Anthony, S.J. O'Day, G. Frenette, A.C. Pavlick, B. Jones, M. Uprichard, and J. Nemunaitis. 2009b. Phase II assessment of talabostat and cisplatin in second-line stage IV melanoma. *BMC Cancer.* 9:263. http://dx.doi.org/10.1186/1471-2407-9-263

Feig, C., A. Gopinathan, A. Neesse, D.S. Chan, N. Cook, and D.A. Tuveson. 2012. The pancreas cancer microenvironment. *Clin. Cancer Res.* 18: 4266–4276. http://dx.doi.org/10.1158/1078-0432.CCR-11-3114

Garin-Chesa, P., L.J. Old, and W.J. Rettig. 1990. Cell surface glycoprotein of reactive stromal fibroblasts as a potential antibody target in human epithelial cancers. *Proc. Natl. Acad. Sci. USA.* 87:7235–7239. http://dx.doi.org/10.1073/pnas.87.18.7235

Hofheinz, R.D., S.E. al-Batran, F. Hartmann, G. Hartung, D. Jäger, C. Renner, P. Tanswell, U. Kunz, A. Amelsberg, H. Kuthan, and G. Stehle. 2003. Stromal antigen targeting by a humanised monoclonal antibody: an early phase II trial of sibrotuzumab in patients with metastatic colorectal cancer. *Onkologie.* 26:44–48. http://dx.doi.org/10.1159/000069863

Kelly, T., Y. Huang, A.E. Simms, and A. Mazur. 2012. Fibroblast activation protein-α: a key modulator of the microenvironment in multiple pathologies. *Int Rev Cell Mol Biol.* 297:83–116. http://dx.doi.org/10.1016/B978-0-12-394308-8.00003-0

Kraman, M., P.J. Bambrough, J.N. Arnold, E.W. Roberts, L. Magiera, J.O. Jones, A. Gopinathan, D.A. Tuveson, and D.T. Fearon. 2010. Suppression of antitumor immunity by stromal cells expressing fibroblast activation protein-alpha. *Science.* 330:827–830. http://dx.doi.org/10.1126/science.1195300

Lee, J., M. Fassnacht, S. Nair, D. Boczkowski, and E. Gilboa. 2005. Tumor immunotherapy targeting fibroblast activation protein, a product expressed in tumor-associated fibroblasts. *Cancer Res.* 65:11156–11163. http://dx.doi.org/10.1158/0008-5472.CAN-05-2805

Liao, D., Y. Luo, D. Markowitz, R. Xiang, and R.A. Reisfeld. 2009. Cancer associated fibroblasts promote tumor growth and metastasis by modulating the tumor immune microenvironment in a 4T1 murine breast cancer model. *PLoS ONE.* 4:e7965. http://dx.doi.org/10.1371/journal.pone.0007965

Loeffler, M., J.A. Krüger, A.G. Niethammer, and R.A. Reisfeld. 2006. Targeting tumor-associated fibroblasts improves cancer chemotherapy by increasing intratumoral drug uptake. *J. Clin. Invest.* 116:1955–1962. http://dx.doi.org/10.1172/JCI26532

Méndez-Ferrer, S., T.V. Michurina, F. Ferraro, A.R. Mazloom, B.D. Macarthur, S.A. Lira, D.T. Scadden, A. Ma'ayan, G.N. Enikolopov, and P.S. Frenette. 2010. Mesenchymal and haematopoietic stem cells form a unique bone marrow niche. *Nature.* 466:829–834. http://dx.doi.org/10.1038/nature09262

Mishra, P.J., P.J. Mishra, R. Humeniuk, D.J. Medina, G. Alexe, J.P. Mesirov, S. Ganesan, J.W. Glod, and D. Banerjee. 2008. Carcinoma-associated fibroblast-like differentiation of human mesenchymal stem cells. *Cancer Res.* 68:4331–4339. http://dx.doi.org/10.1158/0008-5472.CAN-08-0943

Morikawa, S., Y. Mabuchi, Y. Kubota, Y. Nagai, K. Niibe, E. Hiratsu, S. Suzuki, C. Miyauchi-Hara, N. Nagoshi, T. Sunabori, et al. 2009. Prospective identification, isolation, and systemic transplantation of multipotent mesenchymal stem cells in murine bone marrow. *J. Exp. Med.* 206:2483–2496. http://dx.doi.org/10.1084/jem.20091046

Narra, K., S.R. Mullins, H.O. Lee, B. Strzemkowski-Brun, K. Magalong, V.J. Christiansen, P.A. McKee, B. Egleston, S.J. Cohen, L.M. Weiner, et al. 2007. Phase II trial of single agent Val-boroPro (Talabostat) inhibiting Fibroblast Activation Protein in patients with metastatic colorectal cancer. *Cancer Biol. Ther.* 6:1691–1699. http://dx.doi.org/10.4161/cbt.6.11.4874

Nombela-Arrieta, C., J. Ritz, and L.E. Silberstein. 2011. The elusive nature and function of mesenchymal stem cells. *Nat. Rev. Mol. Cell Biol.* 12:126–131. http://dx.doi.org/10.1038/nrm3049

Ostermann, E., P. Garin-Chesa, K.H. Heider, M. Kalat, H. Lamche, C. Puri, D. Kerjaschki, W.J. Rettig, and G.R. Adolf. 2008. Effective

immunoconjugate therapy in cancer models targeting a serine protease of tumor fibroblasts. *Clin. Cancer Res.* 14:4584–4592. http://dx.doi.org/10.1158/1078-0432.CCR-07-5211

Rettig, W.J., P. Garin-Chesa, H.R. Beresford, H.F. Oettgen, M.R. Melamed, and L.J. Old. 1988. Cell-surface glycoproteins of human sarcomas: differential expression in normal and malignant tissues and cultured cells. *Proc. Natl. Acad. Sci. USA.* 85:3110–3114. http://dx.doi.org/10.1073/pnas.85.9.3110

Rosenberg, S.A. 2012. Raising the bar: the curative potential of human cancer immunotherapy. *Sci. Transl. Med.* 4:ps8. http://dx.doi.org/10.1126/scitranslmed.3003634

Sabatino, M., J. Ren, V. David-Ocampo, L. England, M. McGann, M. Tran, S.A. Kuznetsov, H. Khuu, A. Balakumaran, H.G. Klein, et al. 2012. The establishment of a bank of stored clinical bone marrow stromal cell products. *J. Transl. Med.* 10:23. http://dx.doi.org/10.1186/1479-5876-10-23

Sadelain, M., R. Brentjens, and I. Rivière. 2009. The promise and potential pitfalls of chimeric antigen receptors. *Curr. Opin. Immunol.* 21:215–223. http://dx.doi.org/10.1016/j.coi.2009.02.009

Santos, A.M., J. Jung, N. Aziz, J.L. Kissil, and E. Puré. 2009. Targeting fibroblast activation protein inhibits tumor stromagenesis and growth in mice. *J. Clin. Invest.* 119:3613–3625. http://dx.doi.org/10.1172/JCI38988

Scott, A.M., G. Wiseman, S. Welt, A. Adjei, F.T. Lee, W. Hopkins, C.R. Divgi, L.H. Hanson, P. Mitchell, D.N. Gansen, et al. 2003. A Phase I dose-escalation study of sibrotuzumab in patients with advanced or metastatic fibroblast activation protein-positive cancer. *Clin. Cancer Res.* 9:1639–1647.

Tripathi, M., S. Billet, and N.A. Bhowmick. 2012. Understanding the role of stromal fibroblasts in cancer progression. *Cell Adh Migr.* 6:231–235. http://dx.doi.org/10.4161/cam.20419

Tripodo, C., S. Sangaletti, P.P. Piccaluga, S. Prakash, G. Franco, I. Borrello, A. Orazi, M.P. Colombo, and S.A. Pileri. 2011. The bone marrow stroma in hematological neoplasms—a guilty bystander. *Nat Rev Clin Oncol.* 8:456–466. http://dx.doi.org/10.1038/nrclinonc.2011.31

Welt, S., C.R. Divgi, A.M. Scott, P. Garin-Chesa, R.D. Finn, M. Graham, E.A. Carswell, A. Cohen, S.M. Larson, L.J. Old, et al. 1994. Antibody targeting in metastatic colon cancer: a phase I study of monoclonal antibody F19 against a cell-surface protein of reactive tumor stromal fibroblasts. *J. Clin. Oncol.* 12:1193–1203.

Wen, Y., C.T. Wang, T.T. Ma, Z.Y. Li, L.N. Zhou, B. Mu, F. Leng, H.S. Shi, Y.O. Li, and Y.Q. Wei. 2010. Immunotherapy targeting fibroblast activation protein inhibits tumor growth and increases survival in a murine colon cancer model. *Cancer Sci.* 101:2325–2332. http://dx.doi.org/10.1111/j.1349-7006.2010.01695.x